Bioconjugate Chemistry

Article

pubs.acs.org/bc

Nanodiscs as a Modular Platform for Multimodal MR-Optical Imaging

Christiane E. Carney,[†] Ivan L. Lenov,[‡] Catherine J. Baker,[‡] Keith W. MacRenaris,[†] Amanda L. Eckermann,[†] Stephen G. Sligar,*[,‡] and Thomas J. Meade*[,†]

[†]Department of Chemistry, Molecular Biosciences, Neurobiology, Biomedical Engineering, and Radiology, Northwestern University, 2145 Sheridan Road, Evanston, Illinois 60208, United States

[‡]Department of Biochemistry, 505 South Goodwin Avenue, University of Illinois Urbana−Champaign, Urbana, Illinois 61801, United States

Supporting Information

ABSTRACT: Nanodiscs are monodisperse, self-assembled discoidal particles that consist of a lipid bilayer encircled by membrane scaffold proteins (MSP). Nanodiscs have been used to solubilize membrane proteins for structural and functional studies and deliver therapeutic phospholipids. Herein, we report on tetramethylrhodamine (TMR) tagged nanodiscs that solubilize lipophilic MR contrast agents for generation of multimodal nanoparticles for cellular imaging. We incorporate both multimeric and monomeric Gd(III)-based contrast agents into nanodiscs and show that particles containing the monomeric agent (**ND2**) label cells with high efficiency and generate significant image contrast at 7 T compared to nanodiscs containing the multimeric agent (**ND1**) and Prohance, a clinically approved contrast agent.

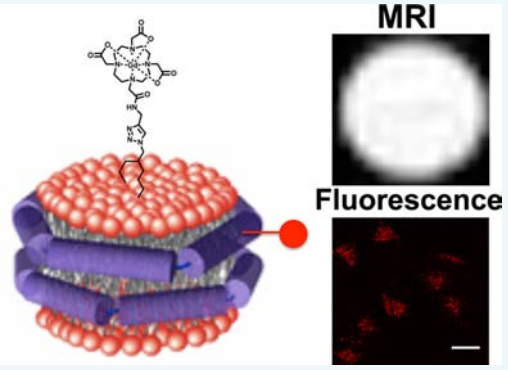

INTRODUCTION

The ability to noninvasively image cells in vivo is essential for applications that include fate mapping transplanted cells,[1−3] cancer detection,[4] tracking gene expression,[5−7] and detecting disease markers.[8−10] Modalities for in vivo imaging include optical techniques, ultrasound, positron emission tomography (PET), single-photon emission computed tomography (SPECT), computed tomography (CT), and magnetic resonance imaging (MRI). MRI is well suited for longitudinal studies and cell tracking since it does not use ionizing radiation or radioactive tracers and provides excellent soft tissue contrast with high temporal resolution.[11] Contrast agents are frequently used to enhance intrinsic MR signal with Gd(III) complexes being the most commonly used in the clinic.[12] These agents generate positive image contrast by decreasing the proton spin−lattice relaxation time (T_1) of water protons.[13] One disadvantage of using Gd(III) agents for cell labeling applications is their relatively low sensitivity which necessitates the use of high concentrations of agent to generate appreciable image contrast.[12]

One strategy to improve the sensitivity of Gd(III) agents is incorporation of contrast agents into nanoparticles. Nanoparticle platforms offer a number of advantages for cell labeling applications including high Gd(III) payload per particle, modular syntheses for generation of multimodal and targeted particles, and an increase in contrast agent relaxivity (efficacy) due to reduced molecular tumbling rates.[14] A number of metal-based nanoparticles have been used as MR contrast agents;[15−17] however, these nanomaterials have been linked to toxicity through mechanisms such as ion release and reactive oxygen species generation.[18−20] As an alternative, biocompatible lipid-based particles including liposomes and high-density lipoprotein (HDL) particles have been investigated as platforms for MR imaging.[21−23] These nanoparticles have been used to label cells[24] and image tumors[25] and atherosclerosis in vivo.[26] Herein, we further develop lipid-based nanoparticles for MR imaging by using nanodiscs than have enhanced stability compared to liposomes and HDL particles.[27]

Nanodiscs are monodisperse, self-assembled discoidal particles that serve as cell membrane mimics.[28,29] They consist of a phospholipid bilayer stabilized by a pair of amphipathic, helical membrane scaffold proteins (MSP) derived from human apolipoprotein A-I. Nanodiscs have been used to solubilize various membrane proteins for structural and functional studies[30] as well as to deliver therapeutic phospholipids to inhibit respiratory syncytial virus (RSV) infection in vitro and in vivo.[31] Additionally, the modular design of nanodiscs allows for facile incorporation of alternate phospholipids, MSPs, targeting groups, and fluorophores.

Herein, we present the synthesis and characterization of tetramethylrhodamine (TMR) tagged-nanodiscs loaded with multimeric and monomeric lipophilic MR contrast agents. We previously reported on Gd(III) chelates conjugated to alkyl chains that had limited solubility in water and required the use of detergent for biological applications.[32] Now, these agents are incorporated into nanodiscs to generate water-soluble nano-

Received: February 23, 2015
Revised: March 30, 2015
Published: April 1, 2015

DOI: 10.1021/acs.bioconjchem.5b00107
Bioconjugate Chem. 2015, 26, 899−905

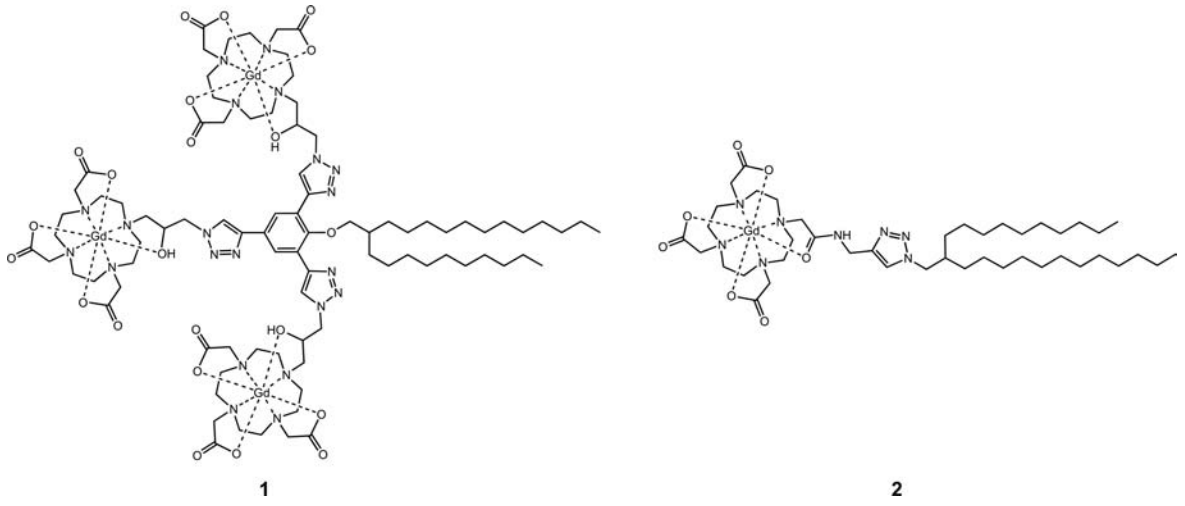

1 2

Figure 1. Structures of lipophilic contrast agents for incorporation into nanodiscs. Complex **1** is multimeric and contains three Gd(III) chelates, while **2** is monomeric and contains a single Gd(III) chelate.

Scheme 1. Nanodiscs Were Synthesized to Contain Varied Amounts of Complex 1 (ND1) or 2 (ND2)[a]

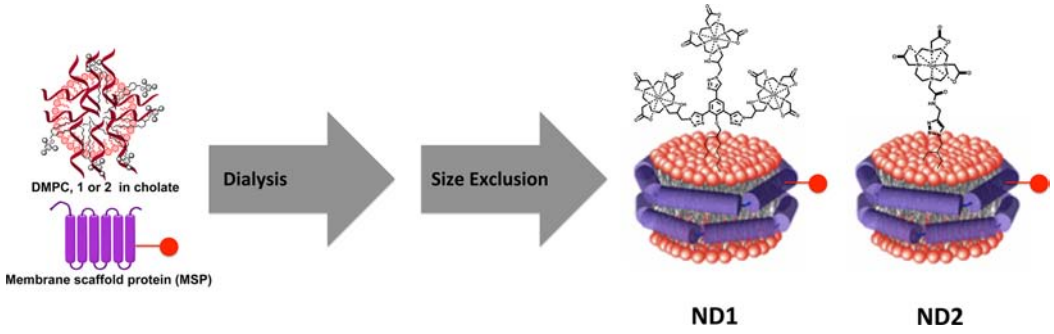

[a]Nanodiscs were prepared by combining DMPC phospholipids, **1** or **2**, and TMR-tagged MSP in cholate. The cholate was removed and the nanodiscs were purified with size exclusion chromatography.

Table 1. Loading and Relaxivities at 1.41 T (37 °C) and 7 T (25 °C) of ND1 and ND2[a]

	loading (%)	Gd(III)/ disc	ionic r_1 (per Gd(II), mM^{-1} s^{-1}), 1.41 T	ionic r_1 (per Gd(III), mM^{-1} s^{-1}), 7 T	molecular r_1 (per ND, mM^{-1} s^{-1}), 1.41 T	molecular r_1 (per ND, mM^{-1} s^{-1}), 7 T
ND1	28 ± 1	137 ± 14	16 ± 1	3.1 ± 0.1	2200 ± 220	430 ± 40
ND2	30 ± 5	48 ± 8	18 ± 1	4.2 ± 0.2	860 ± 140	200 ± 10

[a]Values represent an average from two independently synthesized batches of nanodiscs ± standard deviation of the mean.

particles that label cells with high efficiency and produce significant contrast enhancement at 7 T.

RESULTS AND DISCUSSION

We previously reported on the ability of multimeric and monomeric Gd(III)-based lipophilic MR contrast agents to label cells with high efficiency; however, the agents were limited by poor water solubility and required detergent for use in cell culture.[32] Herein, we incorporate lipophilic contrast agents **1** and **2** into nanodiscs to generate water-soluble, multimodal, and modular platforms for cellular imaging (Figure 1).

Multimeric **1** was synthesized according to literature procedures and contains three Gd(III) chelates.[32] Monomeric **2** was synthesized according to Scheme S1. Specifically, 2-decyltetradecan-1-ol was brominated with NBS to yield 11-(bromomethyl)tricosane. This product was reacted with NaN_3 at 70 °C in DMF to yield 11-(azidomethyl)tricosane which was subsequently reacted with an alkyne modified complex **3** (prepared according to literature procedure)[33] in 2:1 tBuOH:H_2O with $CuSO_4$ and sodium ascorbate to afford the final product **2**.

Complexes **1** and **2** were incorporated into tetramethylrhodamine (TMR) tagged nanodiscs according to Scheme 1. Specifically, MSP was labeled with TMR at Cys73. The tagged MSP was combined with a cholate-solubilized solution of DMPC phospholipids and either **1** or **2** at molar ratios of 1:(90 − *X*):180:*X* (MSP:lipid:cholate:variable amount of **1** or **2**). The cholate was removed with biobeads and the resultant nanodiscs were purified on a size-exclusion chromatography column calibrated with four protein standards. Based on the calibration, the retention time for nanodiscs with a diameter of ∼10 nm is ∼25 min.

The maximum loading of complexes **1** and **2** into nanodiscs was determined by synthesizing particles with varied molar ratios of **1** (**ND1**) and **2** (**ND2**). For both constructs, a maximum of 30% contrast agent loading relative to total lipid content (i.e., phospholipids + **1** or **2**) was achieved (Table S1).

DOI: 10.1021/acs.bioconjchem.5b00107
Bioconjugate Chem. 2015, 26, 899−905

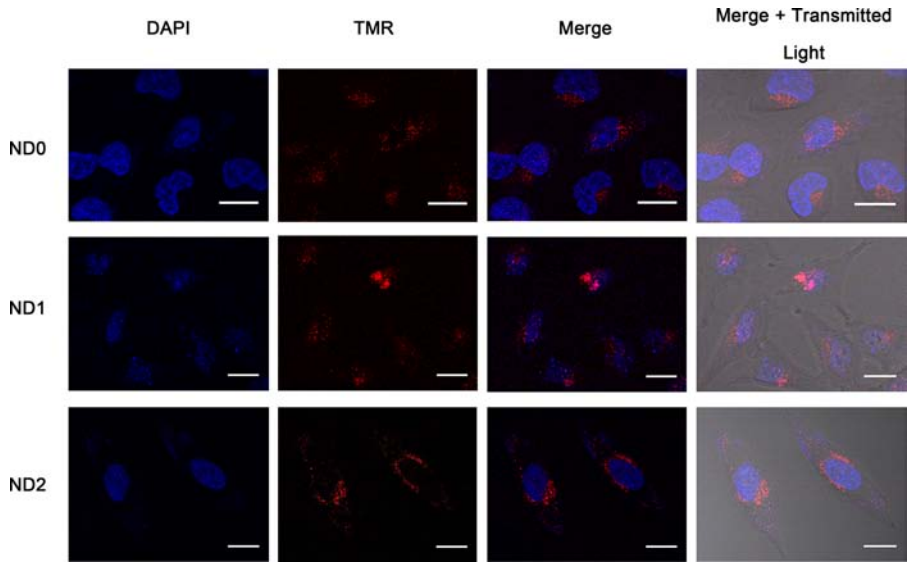

Figure 2. Confocal micrographs of HeLa cells incubated with 1 μM of **ND0**, **ND1**, and **ND2** show intracellular accumulation. Blue = DAPI, Red = TMR. Scale bar = 20 μm.

Consequently, the loading percentages correspond to 137 ± 14 Gd(III) ions per nanodisc for **ND1** and 48 ± 8 for **ND2** (Table 1). These values represent an increase in Gd(III) loading on lipid-based particles with similarly sized HDL particles achieving only 22 Gd(III)/particle.[26] Relaxivity was determined at low (1.41 T) and high (7 T) magnetic field strengths. Both **ND1** and **ND2** have relaxivities of 17 mM^{-1} s^{-1} at 1.41 T (37 °C), which is comparable to other lipid-based particles that typically report relaxivities of 10−30 mM^{-1} s^{-1}.[22] Relaxivities at 7 T (25 °C) are 3.1 mM^{-1} s^{-1} ± 0.1 for **ND1** and 4.2 mM^{-1} s^{-1} ± 0.2 for **ND2**. Additionally, nanodiscs were determined to be stable in buffer for at least 2 weeks and in cell media for at least 1 week (Figure S5).

The ability of **ND1** and **ND2** to label cells was investigated with HeLa and MCF7 cells. All experiments were performed with a 24 h incubation time at concentrations that maintained ≥90% cell viability (Figure S6). Confocal laser scanning microscopy was used to determine cellular localization of TMR-tagged MSP. Micrographs showed intracellular accumulation of the nanodiscs (Figure 2, see SI for *z*-stacks). The localization of **ND1** and **ND2** was compared to that of nanodisc controls without Gd(III) contrast agent (**ND0**). From these micrographs, it does not appear that incorporation of **1** and **2** into nanodiscs significantly affects intracellular accumulation. As complexes **1** and **2** are not covalently attached to the TMR-tagged MSP, the localization of these contrast agents was determined using cell fractionation (Figure 3). Briefly, the membrane and cytosol of the cells were separated and analyzed for Gd(III) content by ICP-MS. These data show that both **1** and **2** show approximately 7-fold greater accumulation in the membrane compared to the cytosol. This suggests that the lipids within the nanodiscs are dynamic and can undergo exchange with lipids in the cell membrane.

Cellular uptake was investigated using flow cytometry for semiquantitative evaluation of fluorescence labeling and ICP-MS for absolute quantification of Gd(III) content. For flow cytometry, cells incubated with 0−1 μM of **ND0**, **ND1**, and **ND2** showed a concentration-dependent increase in fluorescence (Figure S8). Cells labeled with **ND2** showed the greatest fluorescence compared to cells incubated with the same concentration of **ND0** and **ND1**, indicating that **ND2** is the most effective at labeling cells.

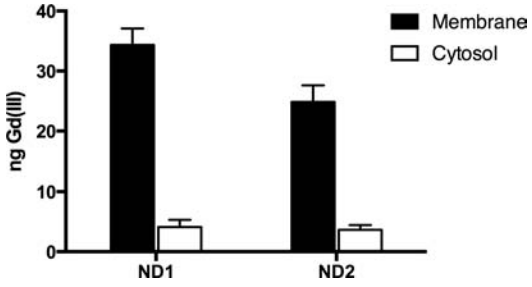

Figure 3. Localization of **1** and **2** was determined using cell fractionation and showed greater accumulation of the contrast agents in the cell membrane compared to the cytosol. These results suggest that the lipids in the nanodiscs can undergo exchange with lipids in the cell membrane.

Evaluation of uptake with ICP-MS validated the results observed with flow cytometry. To account for differences in labeling that may arise from cell line selection, both HeLa and MCF7 were used in uptake experiments. In both cell lines, the labeling achieved was the same for **ND1** and **ND2** when cells were incubated with equalized nanodisc concentration below 0.3 μM despite 3-fold higher Gd(III) per nanodisc loading for **ND1** (Figure 4A). Above incubations of 0.3 μM nanodisc concentration, small variations in labeling of 0.1−0.3 fmol Gd(III) per cell were observed. For cells incubated with equalized Gd(III) concentrations, **ND2** attains labeling approximately 3-fold and 1.6-fold greater than **ND1** in HeLa and MCF7 cells, respectively. The maximum labeling achieved for **ND2** is 4.4 fmol Gd(III) per cell in HeLas and 2.2 fmol Gd(III) per cell in MCF7s (Figure 4B). While **ND1** labels both HeLa and MCF7 cells with similar efficiency, the labeling of **ND2** is approximately 2-fold greater in HeLa cells. This indicates that the labeling of **ND2** is influenced by cell line selection. Overall, these results indicate that nanodiscs loaded with monomeric lipophilic contrast agents attain higher cell labeling than those containing multimeric agents which is consistent with our previous work on lipophilic contrast

DOI: 10.1021/acs.bioconjchem.5b00107
Bioconjugate Chem. 2015, 26, 899−905

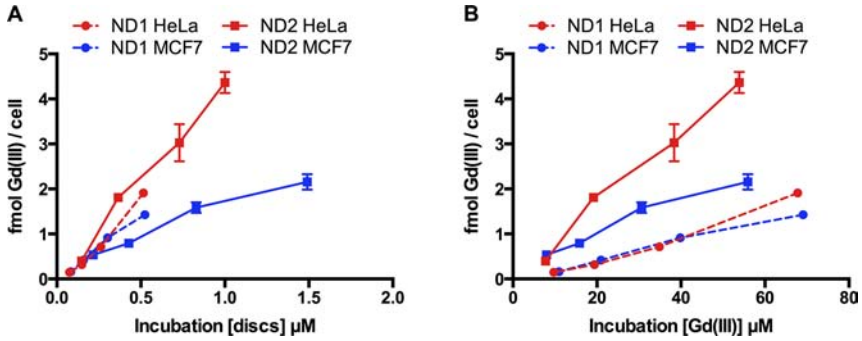

Figure 4. Cell uptake of **ND1** and **ND2** was determined in HeLa (red) and MCF7 (blue) cells at varied incubation concentrations. (A) Uptake at variable nanodisc incubation concentrations shows the same labeling for **ND1** and **ND2**. (B) Uptake at variable Gd(III) incubation concentrations shows that **ND2** attains higher cell labeling. Error bars represent the standard deviation of triplicate experiments.

agents.[32] Further, these results represent an improvement over our previous MR-optical agents that attained labeling of only 1 fmol Gd(III) per cell or less.[34,35]

To investigate the ability of nanodiscs to enhance T_1-weighted contrast of cell populations, MR images of HeLa cell pellets were acquired at 7 T (Figure 5). Cells were labeled with

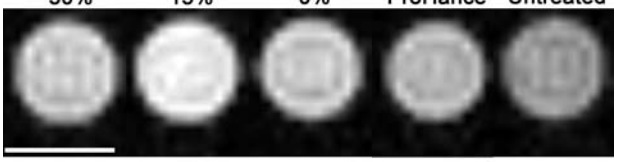

	30%	15%	0%	ProHance®	Untreated
fmoles Gd(III) per cell	1.37	1.08	0.00*	0.05	0.00*
T_1 (ms)	1582 ± 97	1710 ± 124	2501 ± 227	2254 ± 223	2465 ± 257

Figure 5. T_1-weighted MR images at 7 T of HeLa cell pellets labeled with **ND0**, **ND1**, **ND2**, and ProHance. Scale bar represents 1 mm. Error bars represent the standard deviation of the mean of 4 slices. TE = 11 ms, TR = 500 ms, MTX = 256 × 256. These images show that at incubation concentrations of 30 μM Gd(III), **ND2** produces the greatest image contrast.

ND0 (0.6 μM), **ND1** (0.2 μM, 30 μM Gd(III)), **ND2** (0.6 μM, 30 μM Gd(III)), and clinically approved ProHance (30 μM). The most significant contrast enhancement was observed in cells treated with **ND2** with a 66% reduction of T_1 compared to untreated cells followed by **ND1** with a 25% reduction. As expected, no significant contrast enhancement was observed with cells treated with **ND0** or ProHance. These results are consistent with the cell labeling trends observed in Figure 4; however, the fmol Gd(III) per cell values are approximately 2-fold higher in the cell pellets than expected. This may be attributed to differences in cell density between the labeling experiments described in Figure 4 and the cell pellets. Overall, these results validate **ND2** as a promising construct for cellular imaging applications.

Cellular proliferation and retention was measured in HeLa and MCF7 cells. Specifically, cells were labeled with **ND1**, **ND2**, and ProHance, replated in fresh media (t = 0), and allowed to proliferate for 72 h. At the end of the experiment, cells were counted and analyzed for Gd(III) content. Additionally, the media was analyzed for Gd(III) content at 4, 24, 48, and 72 h postlabeling. Cells labeled with **ND1** and **ND2** showed no significant decrease in cellular proliferation compared to cells labeled with ProHance (Figure 6A). In HeLa cells, **ND1** was retained most effectively with 70% of the original label remaining after 72 h of leaching followed by **ND2** with 40% remaining, and ProHance with 20% remaining (Figure 6B). The retention in MCF7 cells was reduced to 50% remaining for **ND1** and 30% for **ND2** (Figure 6C). The retention of ProHance increased to 20% remaining after 72 h of leaching.

The enhanced cellular retention of **ND1** in both cell lines suggests that these nanoparticles may be used for cell tracking applications where it is critical that contrast agents remain associated with cells for long time periods. Examples of such applications include fate-mapping transplanted stem cells and monitoring developmental events. The limited retention of **ND2** indicates that these nanoparticles are better suited for applications where clearance of the contrast agent is desired such as detection of cancer and disease markers. Therefore, nanodiscs may be tailored to specific imaging applications by altering the lipophilic contrast agent incorporated into the particles.

CONCLUSIONS

We have incorporated multimeric and monomeric lipophilic MR contrast agents into TMR-tagged nanodiscs to generate multimodal agents for cellular imaging. Nanodiscs containing multimeric **1** (**ND1**) achieved 3-fold higher Gd(III)/disc loading than those containing monomeric **2** (**ND2**). Despite this advantage in loading, **ND1** did not label cells as effectively as **ND2**. Cellular retention studies showed that 50% or greater of the initial **ND1** label remained associated with cells for 72 h, whereas **ND2** leached from cells more effectively. This indicates that **ND1** may be useful for long-term cell tracking while **ND2** is more appropriate for applications that require rapid clearance of the contrast agent. Additionally, we showed that **ND2** produced significant contrast enhancement of cell populations at 7 T indicating that these nanoparticles may be useful for future in vivo applications. Further, the modular design of nanodiscs will allow for incorporation of targeting groups and alternate fluorophores in future work.

MATERIALS AND METHODS

Synthesis. Complexes **1**,[32] **3**,[33] and **4**[36] were synthesized according to literature procedures. For a description of synthetic methods for new compounds, see the Supporting Information.

Labeling MSP with Tetramethylrhodamine (TMR). MSP labeling was carried out in standard disc buffer (SDB)

DOI: 10.1021/acs.bioconjchem.5b00107
Bioconjugate Chem. 2015, 26, 899−905

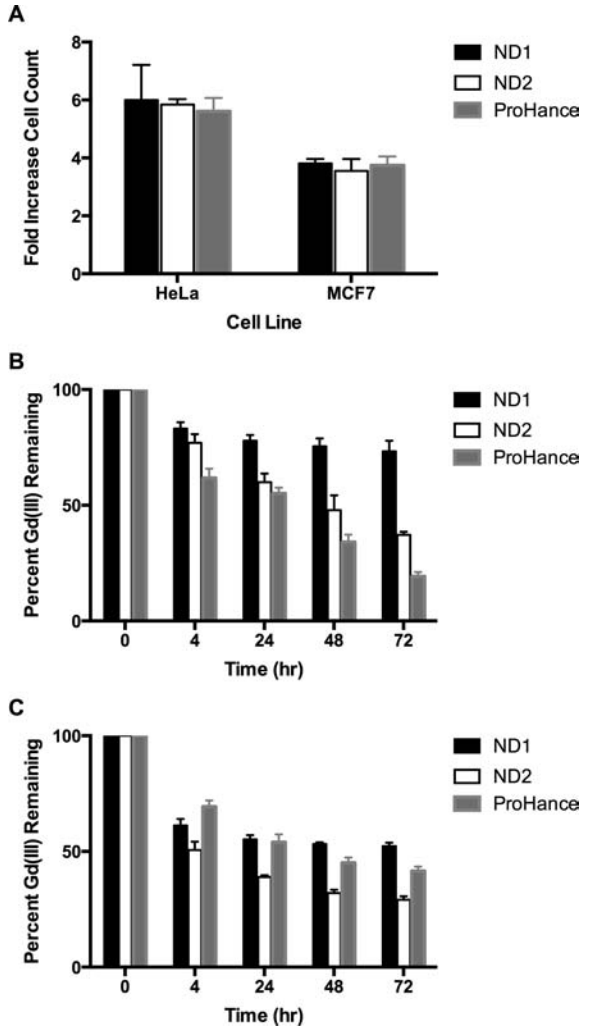

Figure 6. Cellular proliferation and retention of HeLa and MCF7 cells treated with concentrations of **ND1** (45 μM Gd(III)), **ND2** (25 μM Gd(III)), and ProHance (2 mM) chosen to equalize cell labeling. (A) Cellular proliferation was measured as the fold increase in cell number between time = 0 and 72 h. No significant change in proliferation was observed. (B) Cellular retention in HeLa cells was determined by measuring the Gd(III) content in the media at 4, 24, 48, and 72 h postlabeling. **ND1** shows the greatest retention in HeLa cells. (C) Cellular retention was also determined in MCF7 cells. Similar retention was observed for **ND1** and ProHance while **ND2** was retained least effectively by cells. Error bars represent ± the standard deviation of triplicate experiments.

(50 mM Tris/HCl pH 7.4, 0.3 M NaCl). A variant of the membrane scaffold protein MSP1D1 with the 73rd residue mutated from aspartic acid to cysteine (MSP1D1_D73C) was expressed and purified as previously described.[28,29] MSP1D1_D73C was reconstituted to a concentration of 100 uM in SDB. Sodium cholate was added with a final concentration of 10 uM. TMR (Anaspec, Fremont, CA, USA) was dissolved in dimethyl sulfoxide (DMSO). MSP1D1_D73C was reduced with 4 mol equiv of tris(2-carboxyethyl)phosphine (TCEP) and incubated at room temperature for 15 min. TMR was added to the reduced MSP1D1_D73C so that the final concentration was 1 mM. The MSP1D1_D73C/TMR solution was incubated at room temperature for 4 h and then for 16 h at 4 °C. The next day, 1 vol equiv of XAD2 Biobeads (Amberlite) was added to the solution and shaken at room temperature for 4 h. Excess dye was completely removed on a G-25 column. Concentration of MSP1_D73C labeled with TMR was measured spectrophotometrically using 280 nm total protein absorption and using a correction factor of 0.3 at this wavelength of maximum absorbance to account for the absorption of the TMR dye.

Incorporating Complexes 1 and 2 into Nanodiscs. Complexes **1** and **2** were dissolved in chloroform at concentrations of 10 mM. 1,2-dimyristoyl-*sn*-glycero-3-phosphocholine (DMPC) phospholipids (Avanti Polar Lipids, Alabaster, AL, USA) were used as received. The general self-assembly procedure is as described previously.[29] Briefly, desired ratios of lipids and either **1** or **2** were pipetted out into a glass tube, mixed together, and dried under N_2. The lipid/chelate mixture was further dried in a vacuum desiccator for 16 h. The mixture was reconstituted with 0.1 M sodium cholate so that the final concentration of sodium cholate would be twice that of the total lipid/chelate concentration. Labeled MSP1D1_D73C was added to the mixture in a ratio of 90:1 lipid:protein. The mixture was incubated at 25 °C for 20 min before adding XAD2 Biobeads. The reconstitution mixture was incubated at 25 °C for 16 h. The biobeads were removed using a disposable column and then the nanodiscs were purified using a Superdex 200 column (GE Healthcare, Piscataway, NJ, USA). Total nanodisc concentration was measured using a 660 nm Protein Assay (Pierce Biotechnology, Rockford, IL, USA).

Low Field (1.41 T) Relaxivity and Stability. For relaxivity measurements, solutions of **ND1** and **ND2** were prepared in 20 mM Tris buffer (pH 7.4). T_1 and T_2 were determined on a Bruker mq60 minispec NMR spectrometer at 1.41 T (60 MHz) and 37 °C using an inversion recovery pulse sequence with 4 averages, 15 s repetition time, and 10 data points (Bruker Canada; Milton, Ontario, Canada).). For stability measurements, solutions of **ND1** and **ND2** were prepared in either 20 mM Tris buffer or minimum essential media supplemented with 10% fetal bovine serum. T_1 was recorded over a varied time course to monitor stability. Between measurements, the solutions were stored at 4 °C.

General Cell Culture Methods. HeLa cells (ATCC CCL-2) were purchased from the American Type Culture Collection (Manassas, VA, USA) and cultured in phenol red free minimum essential media (MEM) supplemented with 10% fetal bovine serum (FBS). MCF7 cells (ATCC HTB-22) were cultured in phenol red free RPMI-1640 media supplemented with 10% FBS. Cells were grown in a humidified incubator operating at 37 °C and 5.0% CO_2 and harvested with 0.25% TrypLE. Nanodiscs were filtered with 0.2 μm sterile filters prior to incubation with cells.

Confocal. 25 000 HeLa cells were plated on a 35 mm FluoroDish (World Precision Instruments, Sarasota, FL, USA). Cells were incubated with 1 μM of **ND0**, **ND1**, and **ND2** (500 μL) for 24 h. Cells were rinsed ten times with 500 μL of DPBS followed by addition of 1 mL fresh media and 1 μM DAPI (Life Technologies, Carlsbad, CA, USA) for 15 min. The media was aspirated and 500 μL of fresh media were added. Images were acquired on a computer-controlled (via Zen 2009 software) Zeiss LSM 510 confocal laser scanning inverted microscope equipped with a mode-locked Mai Tai DeepSee Ti:sapphire two-photon laser (Spectra Physics, Mountain View, CA, USA). For all images a Plan-Appochromat 40×/1.20NA water immersion Korr UV−vis-IR M27 objective lens with a numerical aperture of 1.2 was used. A multitrack acquisition was used for DAPI and Nanodisc excitation. Track 1: Excitation

DOI: 10.1021/acs.bioconjchem.5b00107
Bioconjugate Chem. 2015, 26, 899−905

of **ND0**, **ND1**, and **ND2** was accomplished with a 543 nm wavelength HeNe laser using a HFT 543/KP700 beamsplitter. The emission from complex **1** was passed through a NFT 545 dichroic and imaged with a PMT through a LP560 nm long-pass filter (1.13 Airy Unit pinhole). Track 2: Excitation of DAPI was accomplished using a software tunable two-photon laser tuned to 755 nm operating at 2.5% laser power, through a HFT 543/KP700 beamsplitter. The emission from DAPI was passed through a NFT 545 dichroic and imaged with a PMT through a 435−485 nm IR bandpass filter. All images were acquired at 512 × 512 resolution and 4 averages. Additionally, *z*-stacks were acquired using the same parameters with 21 slices. Image processing and analysis was performed using *ImageJ* (NIH, Bethesda, MD, USA).

Cell Fractionation. The mechanism of cell labeling was further studied using cell fractionation. 250 000 HeLa cells were seeded in a 6-well plate. Cells were incubated with **ND1** and **ND2** for 24 h. Cells were washed twice with 500 μL DPBS and pelleted at 1000*g* for 5 min at 4 °C. The cytosol and membrane fractions of the cells were separated using a BioVision FractionPREP Cell Fractionation kit (Milpitas, CA, USA) according to the manufacture's protocol. Each fraction was analyzed for Gd(III) content by ICP-MS.

Flow Cytometry. Cell labeling efficiency was assessed with flow cytometry using a BD LSRII (BD Biosciences, San Jose, CA, USA). 40 000 HeLa cells were seeded in a 24-well plate. Cells were incubated with 180 μL of 0−1 μM (disc concentration) **ND0**, **ND1**, and **ND2** for 24 h. Cells were washed twice with 500 μL DPBS, pelleted at 1000*g* for 5 min at 4 °C, suspended in 500 μL of DPBS, and assessed with flow cytometry. Dot plots were gated based upon FSC/SSC properties of unlabeled HeLa cells. Data was analyzed with *FlowJo* software.

Cell Counting and Viability. In all labeling experiments, a Guava EasyCyte Mini Personal Cell Analyzer (PCA) was used to count cells and determine viability according to the manufacture's protocol. Briefly, cell suspensions were mixed with Guava Viacount to obtain an appropriate dilution factor (approximately 30−100 cells/μL) and analyzed with Viacount software module.

Cell Labeling. Either 25 000 HeLa cells or 30 000 MCF7 cells were seeded in a 24-well plate for labeling experiments. Cells were incubated with **ND1** or **ND2** dissolved in media at concentrations of 0−1 μM (disc concentration) for 24 h (180 μL dose). Cells were washed with 2 × 500 μL DPBS, detached with trypsin, and centrifuged at 1000*g* for 5 min at 4 °C. The media was aspirated and the cells were resuspended in 200 μL media. An aliquot of 50 μL was used for cell counting and 130 μL was used for analysis of Gd(III) content by ICP-MS.

Cellular Proliferation and Retention. Either 50 000 HeLa or 60 000 MCF7 cells were seeded in a 12-well plate. Cells were incubated with varied concentrations of agent chosen to equalize cell labeling: **ND1** 45 μM Gd(III), **ND2** 25 μM Gd(III), and ProHance 2 mM (600 μL dose) for 24 h. Cells were detached and processed according to previously published procedures[32] with the following exception: after 4, 24, 48, and 72 h the media was collected, centrifuged, and 250 μL was used for analysis by ICP-MS.

ICP-MS. Gd(III) content of solutions and cells was determined with ICP-MS according to a previously established procedure.[32]

High Field (7 T) Relaxivity and Cell Pellet Imaging. MR imaging and T_1 measurements were performed using a Bruker Pharmscan 7 T imaging spectrometer according to previously described methods.[32] Briefly, a rapid-acquisition rapid-echo (RARE-VTR) T_1-map pulse sequence, with static TE (11 ms), variable TR (150, 250, 500, 750, 1000, 2000, 4000, 6000, 8000, and 10000 ms) values, field of view (FOV) = 25 × 25 mm^2, matrix size (MTX) = 256 × 256, number of axial slices = 4, slice thickness (SI) = 1.0 mm, and averages (NEX) = 3 was used. Relaxivity at 7 T was determined using serially diluted solutions of **ND1** and **ND2**. Image acquisition and analysis was performed as previously described.[32]

■ ASSOCIATED CONTENT

Supporting Information

Synthesis and characterization of **2** and **5**, nanodisc loading and stability, T_2 relaxivity and cell pellets, cellular toxicity, confocal *z*-stacks, and flow cytometry. This material is available free of charge via the Internet at http://pubs.acs.org.

■ AUTHOR INFORMATION

Corresponding Authors

*E-mail: s-sligar@illinois.edu.

*E-mail: tmeade@northwestern.edu.

Present Address

Amanda L. Eckermann, Department of Chemistry, Hope College, 35 East 12th Street, Holland, Michigan 49422, USA.

Notes

The authors declare no competing financial interest.

■ ACKNOWLEDGMENTS

This work was supported by the National Institutes of Health (NIH grants GM033775 and U54CA151880) and by a National Science Foundation Graduate Research Fellowship (C.C.). Imaging was performed at the Northwestern University Center for Advanced Molecular Imaging generously supported by NCI CCSG P30 CA060553 awarded to the Robert H Lurie Comprehensive Cancer Center. MRI was performed on the 7 T Bruker Pharmscan system purchased with the support of NCRR 1S10RR025624-01. Metal analysis was performed at the Northwestern University Quantitative Bioelemental Imaging Center generously supported by NASA Ames Research Center NNA06CB93G.

■ REFERENCES

(1) Modo, M., Beech, J. S., Meade, T. J., Williams, S. C. R., and Price, J. (2009) A chronic 1 year assessment of MRI contrast agent-labelled neural stem cell transplants in stroke. *Neuroimage 47*, T133−T142.

(2) Modo, M., Roberts, T., Sandhu, J., Brekke, C., Ashioti, M., Meade, T. J., Price, J., and Williams, S. C. R. (2004) In vivo detection of stem cells by magnetic resonance imaging. *Neurobiol. Aging 25*, S19−S19.

(3) Ahrens, E. T., and Bulte, J. W. M. (2013) Tracking immune cells in vivo using magnetic resonance imaging. *Nat. Rev. Immunol. 13*, 755−763.

(4) Weissleder, R. (2006) Molecular imaging in cancer. *Science 312*, 1168−1171.

(5) Massoud, T. F., and Gambhir, S. S. (2003) Molecular imaging in living subjects: seeing fundamental biological processes in a new light. *Gene Dev. 17*, 545−580.

(6) Louie, A. Y., Huber, M. M., Ahrens, E. T., Rothbacher, U., Moats, R., Jacobs, R. E., Fraser, S. E., and Meade, T. J. (2000) In vivo visualization of gene expression using magnetic resonance imaging. *Nat. Biotechnol. 18*, 321−325.

(7) Keliris, A., Ziegler, T., Mishra, R., Pohmann, R., Sauer, M. G., Ugurbil, K., and Engelmann, J. (2011) Synthesis and characterization

DOI: 10.1021/acs.bioconjchem.5b00107
Bioconjugate Chem. 2015, 26, 899−905

of a cell-permeable bimodal contrast agent targeting beta-galactosidase. *Bioorg. Med. Chem. 19*, 2529−40.
(8) Sukerkar, P. A., MacRenaris, K. W., Meade, T. J., and Burdettes, J. E. (2011) A steroid-conjugated magnetic resonance probe enhances contrast in progesterone receptor expressing organs and tumors in vivo. *Mol. Pharmaceut. 8*, 1390−1400.
(9) Sosnovik, D. E., Schellenberger, E. A., Nahrendorf, M., Novikov, M. S., Matsui, T., Dai, G., Reynolds, F., Grazette, L., Rosenzweig, A., Weissleder, R., et al. (2005) Magnetic resonance imaging of cardiomyocyte apoptosis with a novel magneto-optical nanoparticle. *Magn. Reson. Med. 54*, 718−724.
(10) Winter, P. M., Caruthers, S. D., Yu, X., Song, S. K., Chen, J. J., Miller, B., Bulte, J. W. M., Robertson, J. D., Gaffney, P. J., Wickline, S. A., et al. (2003) Improved molecular imaging contrast agent for detection of human thrombus. *Magn. Reson. Med. 50*, 411−416.
(11) Modo, M., Hoehn, M., and Bulte, J. W. M. (2005) Cellular MR imaging. *Mol. Imaging 4*, 143−164.
(12) Caravan, P. (2006) Strategies for increasing the sensitivity of gadolinium based MRI contrast agents. *Chem. Soc. Rev. 35*, 512−523.
(13) Helm, L., Merbach, A. E., and Tóth, E. (2013) *The chemistry of contrast agents in medical magnetic resonance imaging*, 2nd ed., John Wiley & Sons, New York.
(14) Bruckman, M. A., Yu, X., and Steinmetz, N. F. (2013) Engineering Gd-loaded nanoparticles to enhance MRI sensitivity via T(1) shortening. *Nanotechnology 24*, 462001.
(15) Song, Y., Xu, X., MacRenaris, K. W., Zhang, X. Q., Mirkin, C. A., and Meade, T. J. (2009) Multimodal gadolinium-enriched DNA-gold nanoparticle conjugates for cellular imaging. *Angew. Chem., Int. Ed. 48*, 9143−7.
(16) Rieter, W. J., Kim, J. S., Taylor, K. M., An, H., Lin, W., Tarrant, T., and Lin, W. (2007) Hybrid silica nanoparticles for multimodal imaging. *Angew. Chem., Int. Ed. 46*, 3680−2.
(17) Qin, H., Zhou, T., Yang, S. H., Chen, Q., and Xing, D. (2013) Gadolinium(III)-gold nanorods for MRI and photoacoustic imaging dual-modality detection of macrophages in atherosclerotic inflammation. *Nanomedicine (London, U.K.) 8*, 1611−1624.
(18) Sabella, S., Carney, R. P., Brunetti, V., Malvindi, M. A., Al-Juffali, N., Vecchio, G., Janes, S. M., Bakr, O. M., Cingolani, R., Stellacci, F., et al. (2014) A general mechanism for intracellular toxicity of metal-containing nanoparticles. *Nanoscale 6*, 7052−61.
(19) Manke, A., Wang, L., and Rojanasakul, Y. (2013) Mechanisms of nanoparticle-induced oxidative stress and toxicity. *BioMed. Res. Int. 2013*, 942916.
(20) Schrand, A. M., Rahman, M. F., Hussain, S. M., Schlager, J. J., Smith, D. A., and Syed, A. F. (2010) Metal-based nanoparticles and their toxicity assessment. *Wiley Interdiscip. Rev.: Nanomed. Nanobiotechnol. 2*, 544−68.
(21) Langereis, S., Geelen, T., Grull, H., Strijkers, G. J., and Nicolay, K. (2013) Paramagnetic liposomes for molecular MRI and MRI-guided drug delivery. *NMR Biomed. 26*, 728−44.
(22) Mulder, W. J., Strijkers, G. J., van Tilborg, G. A., Griffioen, A. W., and Nicolay, K. (2006) Lipid-based nanoparticles for contrast-enhanced MRI and molecular imaging. *NMR Biomed. 19*, 142−64.
(23) Cormode, D. P., Frias, J. C., Ma, Y. Q., Chen, W., Skajaa, T., Briley-Saebo, K., Barazza, A., Williams, K. J., Mulder, W. J. M., Fayad, Z. A., et al. (2009) HDL as a contrast agent for medical imaging. *Clin. Lipidol. 4*, 493−500.
(24) Mulder, W. J. M., Strijkers, G. J., Griffioen, A. W., van Bloois, L., Molema, G., Storm, G., Koning, G. A., and Nicolay, K. (2004) A liposomal system for contrast-enhanced magnetic resonance imaging of molecular targets. *Bioconjugate Chem. 15*, 799−806.
(25) Kamaly, N., Kalber, T., Kenny, G., Bell, J., Jorgensen, M., and Miller, A. (2010) A novel bimodal lipidic contrast agent for cellular labelling and tumour MRI. *Org. Biomol. Chem. 8*, 201−211.
(26) Chen, W., Vucic, E., Leupold, E., Mulder, W. J. M., Cormode, D. P., Briley-Saebo, K. C., Barazza, A., Fisher, E. A., Dathe, M., and Fayad, Z. A. (2008) Incorporation of an apoE-derived lipopeptide in high-density lipoprotein MRI contrast agents for enhanced imaging of macrophages in atherosclerosis. *Contrast Media Mol. Imaging 3*, 233−242.
(27) Kleinschmidt, J. H. (2013) *Lipid-protein interactions: methods and protocols*, Springer, New York.
(28) Denisov, I. G., Grinkova, Y. V., Lazarides, A. A., and Sligar, S. G. (2004) Directed self-assembly of monodisperse phospholipid bilayer nanodiscs with controlled size. *J. Am. Chem. Soc. 126*, 3477−3487.
(29) Bayburt, T. H., Grinkova, Y. V., and Sligar, S. G. (2002) Self-assembly of discoidal phospholipid bilayer nanoparticles with membrane scaffold proteins. *Nano Lett. 2*, 853−856.
(30) Nath, A., Atkins, W. M., and Sligar, S. G. (2007) Applications of phospholipid bilayer nanodiscs in the study of membranes and membrane proteins. *Biochemistry 46*, 2059−2069.
(31) Numata, M., Grinkova, Y. V., Mitchell, J. R., Chu, H. W., Sligar, S. G., and Voelker, D. R. (2013) Nanodiscs as a therapeutic delivery agent: inhibition of respiratory syncytial virus infection in the lung. *Int. J. Nanomed. 8*, 1417−1427.
(32) Carney, C. E., MacRenaris, K. W., Mastarone, D. J., Kasjanski, D. R., Hung, A. H., and Meade, T. J. (2014) Cell labeling via membrane-anchored lipophilic MR contrast agents. *Bioconjugate Chem. 25*, 945−954.
(33) Song, Y., Kohlmeir, E. K., and Meade, T. J. (2008) Synthesis of multimeric MR contrast agents for cellular imaging. *J. Am. Chem. Soc. 130*, 6662−+.
(34) Song, Y., Xu, X. Y., MacRenaris, K. W., Zhang, X. Q., Mirkin, C. A., and Meade, T. J. (2009) Multimodal gadolinium-enriched DNA-gold nanoparticle conjugates for cellular imaging. *Angew. Chem., Int. Ed. 48*, 9143−9147.
(35) Brekke, C., Morgan, S. C., Lowe, A. S., Meade, T. J., Price, J., Williams, S. C. R., and Modo, M. (2007) The in vitro effects of a bimodal contrast agent on cellular functions and relaxometry. *NMR Biomed. 20*, 77−89.
(36) Li, H. R., Sun, S. Y., Salim, T., Bomma, S., Grimsdale, A. C., and Lam, Y. M. (2012) Conjugated polymers based on dicarboxylic imide-substituted isothianaphthene and their applications in solar cells. *J. Polym. Sci.: Polym. Chem. 50*, 250−260.

DOI: 10.1021/acs.bioconjchem.5b00107
Bioconjugate Chem. 2015, 26, 899−905